

Dosimetric Characteristics of a Newly Designed Grid Block for Megavoltage Photon Radiation and Its Therapeutic Advantage Using A Linear Quadratic Model

Ali S. Meigooni, Kai Dou, Navid J. Meigooni, Michael Gnaster, Shahid Awan, Sharifeh Dini, and Ellis L. Johnson

University of Kentucky Chandler Medical Center
Department of Radiation Medicine
Lexington, Kentucky 40536-0084

Submitted to Medical Physics Journal on March 6, 2006. Revised on 5/22/2006. The second revision on 6/29/2006.

Corresponding Author:

Ali S. Meigooni, Ph.D.
University of Kentucky Medical Center
Department of Radiation Medicine
800 Rose Street
Lexington KY, 40536-0084
Tel: (859) 323-6486
Fax: (859) 257-1211
Email: alimeig@uky.edu

Abstract

Grid radiation therapy with megavoltage x-ray beam has been proven to be an effective technique for management of large, bulky malignant tumors. The clinical advantage of GRID therapy, combined with the conventional radiation therapy, has been demonstrated using a prototype GRID block¹. Recently, a new GRID block design with improved dosimetric properties has become commercially available from the Radiation Product Design, Inc. (5218 Barthel Industrial Dr., Albertville, MN). This GRID collimator consists of an array of focused apertures in a Cerrobend block arranged in a hexagonal pattern having a circular cross section diameter and center to center spacing of 14.3 mm and 21.1 mm, respectively, in the plane of isocenter. In this project, dosimetric characteristics of the newly redesigned GRID block have been investigated for a Varian 21EX linear accelerator. These determinations were performed using radiographic films, thermoluminescent dosimeters (TLDs) in Solid WaterTM phantom materials and an ionization chamber in water. The output factor, percentage depth dose, beam profiles, and isodose distributions of the GRID radiation as a function of field size and beam energy have been measured using both 6 MV and 18 MV x-ray beams. In addition, the therapeutic advantages obtained from this treatment modality with the new GRID block design for a high, single fraction of dose have been calculated using the linear quadratic model with α/β ratios for typical tumor and normal cells. These biological characteristics of the new GRID block design will also be presented.

Key words: Grid therapy, megavoltage photon radiation, dosimetry, cell survival, Therapeutic advantage

I. Introduction

Megavoltage GRID radiation therapy is a new paradigm in the management of bulky (>8 cm) malignant tumors¹⁻⁴. The Department of Radiation Medicine at the University of Kentucky has utilized a modified spatially-fractionated technique with megavoltage X-ray beam for treatment of advanced tumors^{3, 4}. Dosimetric characteristics of these GRID radiation fields for both photon and electron beams have been studied by several investigators.⁵⁻⁷ It is interesting to know that the published clinical results¹⁻⁴ were obtained with a prototype GRID block that was constructed by placing several segments of copper tubing between two plastic trays and filling the space between the tubes with cerrobend material. Therefore, the differences in attenuation between the copper tubing and cerrobend material as well as the non-divergent match problem of the copper tubing to the divergent beam brought about a challenge to the design of the prototype GRID block. Despite the problems mentioned above in the prototype GRID block design, Mohiuddin et al³ have shown that the overall response rate of the patients increased from 62% to 91% when they were treated with a single-field GRID irradiation of ≥ 15 Gy plus conventional external beam therapy.

Recently a new GRID block has been designed and fabricated by the Radiation Product Design, Inc. (5218 Barthel Industrial Dr., Albertville, MN). This block was constructed by casting the divergent holes in a cerrobend block, using a stereotactic method which is able to provide the optimal conditions of: 1) accurate beam divergence, and 2) less transmission through the blocked area. This block design allows for a greater volume of tissue to receive the therapeutic dose of greater than 85%. The hole size and center-to-center spacing can be customized, and also the divergence of the holes can be designed to match one of the commercially available linear accelerators. Characterization of the dosimetric and biological properties of the new GRID block design are necessary for clinical implementation.

While the evaluation of dosimetric properties of GRID irradiation is relatively straight forward, the biological analysis is much more difficult. The radiobiology of GRID irradiation is not well understood and is currently being studied by several investigators^{8, 9}. Proposed mechanisms of action include the production of various cytokines in the irradiated tissues⁹. For a non-uniform radiation field, Niemierko¹⁰ introduced a radiobiological model, based on Linear Quadratic model, to describe the biological effectiveness of the inhomogeneous dose distribution such as 3D conformal therapy. Zwicker et al¹¹ have extended this model to evaluate radiobiological properties of GRID irradiation. They have concluded that for a wide range of tumor tissue sensitivities, a single-dose partial-volume GRID radiation field may have a significant therapeutic advantage over open field radiotherapy in sparing normal tissues.

The goal of this project is to investigate the physical and biological characteristics of the megavoltage photon radiation through this newly designed GRID block for a Varian 21EX linear accelerator. Dosimetric characteristics (i.e. beam profiles, isodose distributions, output factor, and percent depth dose of radiation field) for this BLOCK design were experimentally determined. Measurements were performed for 6 MV and 18 MV x-ray beams using radiographic film and thermoluminescent dosimeters (TLDs) in Solid WaterTM phantom material (Radiation Measurements Inc., RMI, Middleton, WI) and an ionization chamber in water. The biological analysis of the new GRID block utilizes the above mentioned model by Zwicker et al¹¹.

II. Materials and Methods

A. Grid design

The GRID block used in the current experiment was manufactured by Radiation Products Design, Inc. This block was constructed by casting a hexagonal array of divergent holes 14.3 mm in diameter with 21.1 mm center-to-center spacing projected in the plane of isocenter. The apertures were cast in a 7.5 cm thick cerrobend block. The divergence of the holes were designed for a Varian 21EX (Varian Associates,

Palo Alto, CA) linear accelerator having a source-to-tray distance of 65.4 cm. Similar to the prototype GRID block, the new GRID apertures design provides approximately 41.7% open area at isocenter. Various field sizes up to a maximum of 25×25 cm can be achieved with this block design. Fig. 1(a) shows the top view of the GRID block. Fig. 1(b) illustrates the GRID block mounted in the block tray holder of the Varian 21EX linear accelerator.

B. Film dosimetry

Film dosimetry was utilized to obtain beam profiles for the GRID collimated fields using 6 MV and 18 MV photon beams from a Varian Clinac 21EX linear accelerator. The measurements were performed in Solid Water™ phantom materials using the Kodak X-Omat V radiographic film (Eastman Kodak Company, Rochester, NY). The beam profiles were measured along the two orthogonal directions (inplane and crossplane) in a plane perpendicular to the central beam axis. These measurements were performed at depths of d_{max}, 5 cm, and 10 cm in 23 cm thick Solid Water™ phantom material for 6 MV and 18 MV x-ray beams (Fig. 2). The irradiated films were read with a Lumiscan-50 laser scanner (Lumisys, Sunnyvale, CA) and processed with MEPHYSTO software (Version 6.30, PTW-New York Co., Hicksville, New York), Microsoft Excel, and Origin® Version 6.1 (OriginLAB Corp, One Roundhouse Plaza, Northampton, MA). Batch and energy specific calibration curves were used to obtain dose for the measured transmittance. Calibrations were obtained for doses of 1, 5, 10, 20, 30, 50, 60, and 70 cGy using a 10 x 10 cm open field at 100 cm SSD at depth of d_{max} in Solid Water™ phantom material.

C. TLD technique and phantom design

TLD measurements were performed at depths of d_{max}, 5 cm, and 10 cm for both 6 MV and 18 MV x-ray beams using LiF TLD chips (TLD-100, Thermo Electron Corp, Oakwood Village, OH) in Solid Water™ phantom material. This phantom material was accurately machined to accommodate the 1x1x1 mm³ TLD chips at the center of the GRID holes and blocked areas (Fig. 3). The irradiated TLD response was obtained using a Harshaw Model 3500 TLD reader (Thermo Electron Corp, Oakwood Village, OH). The responses of at least 10 TLD chips, from the same batch of TLDs, were calibrated using open radiation field (i.e., 10x10 cm²) with 6 MV x-ray beams. The corresponding responses from the TLDs irradiated in the GRID field were then converted to dose following procedures described by Meigooni et al¹². The mean values of up to 7 chips were used to evaluate each measurement point.

Application of TLD chips for radiation dosimetry in both external beam and brachytherapy fields have been demonstrated by various investigators¹²⁻¹⁶. Equation (1) was used to calculate the absorbed dose rate from the TLD responses for each point irradiated in the phantom¹²:

$$D(d) = \frac{R(d)}{MU \cdot \epsilon \cdot F_{lin}} \quad (1)$$

where $D(d)$ is the absorbed dose per Monitor Unit (MU) at depth of d , R is the TLD response corrected for background and the physical differences between the TLD chips using predetermined chip factors, and MU is the Monitor Unit used for the exposure of TLDs, ϵ is the calibration factor for the TLD response (nC/cGy) measured with a 6 MV or 18 MV X-ray beam from a linear accelerator, and F_{lin} is the nonlinearity correction of the TLD response for the given dose. In these measurements, the absorbed dose exposure level was selected to be in the range of 10 to 100 cGy for which F_{lin} was assumed to be unity¹².

D. Ion chamber measurements

Percent depth dose (PDD) and beam profiles were measured using a Scanditronix Wellhofer 3D radiation scanning system (Scanditronix Wellhofer North America, Bartlett, TN) with a Wellhofer Model CC01 chamber. This microchamber has a sensitive volume of 0.01 cm³ (1 mm radius and 3.6 mm active length). The chamber was scanned in the direction of the chamber diameter, which provides a sufficiently small spatial resolution, relative to the GRID hole diameter (14 mm), for dosimetry of GRID radiation field. These measurements were performed as a function of depth, field size, and beam energy. This system consisted of a standard 48×48×48 cm water tank, Wellhofer Model CU 500E dual channel control unit, and WP 700 software. For output factor measurements, the CC01 ionization chamber charge readings

were obtained with an Invision Model 35040 dosimeter. Output factors were then obtained by calculating the ratio of the average charge readings for a 10x10 cm field without to with GRID block at d_{max} depth and 100 cm SSD.

E. Therapeutic Advantage of GRID therapy

The methodology of Zwicker et al¹¹ has been used to evaluate the potential therapeutic advantage of the newly designed GRID field. The overall survival fraction (SF) is determined from an area weighted average of local SF and is calculated for both normal and tumor cells. Uniform field calculations are also performed for a dose level that gives the same tumor SF in both the open and GRID fields. The therapeutic advantage is then defined as:

$$\text{Therapeutic Advantage} = \frac{SF_{GRID \text{ field}}^{Normal \text{ tissue}}}{SF_{Open \text{ field}}^{Normal \text{ tissue}}}, \quad (2)$$

where each normal-tissue SF is calculated for the same tumor SF. The α/β ratios used for these calculations, 10 Gy for tumor cells and 2.5 Gy for normal cells, represent typical values for these tissue types.

III. Results and Discussion

A. Dosimetric characteristics

To validate the use of different dosimeters in this investigation, the results obtained using TLD, ionization chamber, and film dosimetry were compared in graphical and tabulated formats. Tables 1A and 1B show excellent agreements ($\pm 5\%$) between the three techniques in measuring the output factors for both 6 MV and 18 MV x-ray beams, respectively. Figs. 4(a) and 4(b) show the excellent agreement between the dose profile of 6 MV x-ray measured with film dosimetry technique and those measured with ionization chamber, at d_{max} and 10 cm depths. Similar results were obtained for 18 MV photon beams. With these validations, any of these dosimetric techniques could be utilized for the remainder of these investigations. The output factors of the new GRID block as a function of field size for both 6 MV and 18 MV were measured in water using the ionization chamber (Table 2A). The open field $S_{c,p}$ was compared with GRID relative outputs at d_{max} and 100 cm SSD as a function of field size and energy in Table 2B. These results indicated a good agreement between open field $S_{c,p}$ and GRID output factors for both 6 MV and 18 MV photon beams.

The crossplane beam profiles for the newly redesigned GRID block were compared with that of the prototype grid. These comparisons are shown in Figs. 5(a) and 5(b). These figures show good symmetry and well-patterned dose profiles for both grid designs. However, relative to the prototype grid, the new GRID block shows approximately a 50% dose reduction to the blocked regions of the field for both 6 MV and 18 MV photons. This reduction can be attributed to the differences of beam divergence and attenuation for the two block designs.

Figures 6(a) and 6(b) show the comparison of measured beam profiles using film dosimetry technique for an open 10x10 cm² field versus GRID field for both 6 MV and 18 MV photons, respectively. The dose profiles in these figures were normalized to the central axis dose value of the open field. These figures indicate an output factor of 100% for an open field and 90% for 6 MV GRID field. However the output factors for 18 MV open and GRID fields were found to be 100% and 78%, respectively. These output factors are utilized for treatment planning of patients treated with GRID.

Figs. 7(a) and 7(b) represent the dose distribution and isodose curves of a GRID radiation field for 6 MV photons, respectively. These figures were obtained using film dosimetry technique at depth of d_{max} for a 10x10 cm field. Figure 7(b) shows the minimum contagious isodose lines between the GRID holes were found to be approximately 12-16% which is consistent with TLD and ionization chamber measured data shown in Table 1A. Fig. 8 shows a comparison of crossplane beam profiles for 6 MV and 18 MV photons at d_{max} depth for a 10x10 cm field size measured with ionization chamber. This figure indicates a similar dose profiles for the two photon energies.

Comparisons of GRID field profiles as a function of depth measured with film dosimetry technique for 6 MV and 18 MV photons are shown in Figs. 9 and 10, respectively. Dose profiles at different depths are normalized to the CAX dose at the d_{max} depth for both beam energies. These figures indicate that the dose to the open region (i.e. hole) of the GRID field decreases with increasing depth, but the dose to the blocked area remains nearly constant. Therefore, the ratio of the peak to valley dose decreases with increasing depth.

Figs. 11(a) and 11(b) show the percent depth dose (%DD) of 6 MV and 18 MV GRID field, respectively, along the depth axis of the central aperture. These data were measured with an ionization chamber in water, film dosimetry, and TLD in Solid WaterTM using a 10x10 cm field size and 100 cm SSD. These results indicate an excellent agreement between the data measured with the three different techniques for both 6 and 18 MV x-rays. Figure 12 demonstrates the impact of the field size on the %DD of 6 and 18 MV beam. As shown in this figure, no significant differences (within $\pm 2.5\%$ at the depth of 30 cm) were observed for the 18 MV beam. However, these differences increase to approximately $\pm 10\%$ for 6 MV beam at the depth of 30 cm.

B. Cell survival estimation under GRID field irradiation

The surviving fractions (SF) of tumor and normal cells are expressed by a linear quadratic model for a single uniform dose irradiation in the linear-quadratic model of cell survival. Typical values for the ratio α/β are 10 Gy for tumor cells and 2.5 Gy for normal tissues¹⁷⁻¹⁸. If a cell survival of 0.5 for a dose of 2 Gy is assumed, the resulting values of α and β will be 0.289 and 0.0289 for tumor cells and 0.193 and 0.077 for normal tissues. The therapeutic advantage of GRID irradiation was modeled in terms of the normal tissue cell survival ratio of a GRID versus an open field for the same tumor cell kill¹¹.

Assuming identical dose distribution under each grid hole (Figures 9 and 10) at a given depth, the dose profile under central axis grid hole (Fig. 13a) was utilized to calculate the surviving fraction of the cells as a function of absorbed dose following Zwicker et al's model¹¹. Fig. 13 (b) shows the integral dose area histogram and Figure 13(c) shows the differential dose area histogram used in these calculations. The cell surviving fraction in tissue irradiated by such a dose distribution is determined and the results were utilized for evaluation of the therapeutic advantage of the GRID with Eq. 2. Figure 14 shows the therapeutic advantage determined for tumor cells with $\alpha=0.289$, $\beta=0.0289$, and $\alpha/\beta = 10$ and normal tissue cells with $\alpha=0.193$, $\beta=0.077$, and $\alpha/\beta = 2.5$.

IV. Conclusions

Dosimetric characteristics of a newly redesigned GRID block have been evaluated as a function of field size and beam energy. A dose to the blocked area of the GRID is significantly reduced compared to that obtained with the prototype grid block. The new GRID shows a large dynamic range of dose cross the open and blocked area of the field with the valley-to-peak ratios increasing with increasing beam energy and depth. The field size dependent output factors obtained for the GRID are generally consistent with the previously measured open field output factors for this linear accelerator.

The standard linear quadratic model was employed to evaluate this GRID by studying cell survival and therapeutic advantage up to 30 Gy. On the basis of cell survival with a cell survival of 0.5 for a dose of 2 Gy assumed, large single-dose fraction treatment using GRID is expected to have a remarkably therapeutic advantage over open field treatment to achieve the same level of tumor cell killing. A greater therapeutic advantage of 2.20 is, in particular, predicted with GRID therapy at a 15-Gy grid irradiation versus an open field and the therapeutic gain is found to increase with dose. Dosimetric characteristics of a GRID and corresponding therapeutic advantage of GRID therapy appear to increase credit in this modality for single high-dose GRID radiotherapy.

Acknowledgments

The authors would like to thank Dr. Robert Zwicker for valuable discussions.

References

- 1 M. Mohiuddin, D.L. Curtis, W.T. Grizos, L. Komarnicky, "Palliative treatment of advanced cancer using multiple nonconfluent pencil beam radiation: A pilot study," *Cancer*. **66**, 114-118 (1990).
- 2 M. Mohiuddin, J.H. Steves, J.E. Reiff, M.S. Huq, N. Suntharalingam, "Spatially Fractionated (GRID) Radiation for Palliative Treatment of Advanced Cancer," *Radiation Oncology Investigations*, **4**, 41-47 (1996).
- 3 M. Mohiuddin, M. Fujita, W. F. Regine, A. S. Meigooni, G. S. Ibbott, and M. M. Ahmed, "High-dose spatially fractionated radiation (GRID): A new paradigm in the management of advanced cancers," *Int. J. Radiat. Oncol. Biol. Phys.* **45**, 721-7 (1999).
- 4 M. Mohiuddin, M. Kudrimoti, W.F. Regine, A.S. Meigooni, R. Zwicker, "Spatially Fractionated Radiation (SFR) in the Management of Advanced Cancer," *J Euro Soc Ther Rad Oncol*, **64**, S313 (2002).
- 5 J. E. Reiff, M. S. Hug, M. Mohiuddin, and N. Suntharalingam, "Dosimetric Properties of megavoltage grid therapy," *Int. J. Radiat. Oncol. Biol. Phys.* **33**, 937-42 (1995).
- 6 J. V. Trapp, A. P. Warrington, M. Partridge, A. Philips, J. Glees, D. Tait, R. Ahmed, M. O. Leach, and S. Webb, "Measurement of the three-dimensional distribution of radiation dose in grid therapy," *Phys. Med. and Biol.* **49**, N317-23 (2004).
- 7 A. S. Meigooni, S. A. Parker, J. Zheng, K. J. Kalbaugh, W. F. Regine, and M. Mohiuddin, "Dosimetric characteristics with spatial fractionation using electron GRID therapy," *Medical Dosimetry* **27**, 37-42 (2002).
- 8 B.S. Sathishkumar, B. Boyanovsky, A.A. Karakashian, K. Rozenova, N.V. Giltaiy, M. Mohiuddin, M. Kudrimoti, M.M. Ahmed, M. Nikolova-Karakashian, "Elevated Sphingomyelinase Activity and Ceramide Concentration in Serum of Patients Undergoing High Dose Spatially Fractionated Radiation Treatment: Implications for Endothelial Apoptosis," *Cancer Biol Ther.* **4**, 979-986 (2005).
- 9 B.S. Sathishkumar, S. Dey, A.S. Meigooni, W.F. Regine, M. Kudrimoti, M.M. Ahmed, M. Mohiuddin, "The Impact of TNF- α Induction on Therapeutic Efficacy following High Dose Spatially Fractionated (GRID) Radiation," *Technology in Cancer Research & Treatment* **1**(2), 141-147 (2002).
- 10 A. Niemierko, "Reporting and analyzing dose distribution: A concept of equivalent uniform dose," *Med. Phys.* **24**, 103-110 (1997).
- 11 R. D. Zwicker, A. S. Meigooni, and M. Mohiuddin, "Therapeutic advantage of GRID irradiation for large single fractions," *Int. J. Radiat. Oncol. Biol. Phys.* **58**, 1309-15 (2004).
- 12 A.S. Meigooni, V. Mishra, H. Panth, and J.F. Williamson, "Instrumentation and dosimeter-size artifacts in quantitative thermoluminescence dosimetry of low dose fields," *Med. Phys.* **22**, 555-61 (1995).
- 13 I. Gomola, J. Van Dam, J. Isern-Verdum, J. Verstraete, R. Reymen, A. Dutreix, B. Davis, D. Huyskens, "External audits of electron beams using mailed TLD dosimetry: preliminary results," *Radiother Oncol.* **58**, 163-8 (2001).
- 14 A. S. Meigooni, K. Sowards, and M. Soldano, "Dosimetric characteristics of the InetrSource ¹⁰³ palladium brachytherapy sources," *Med. Phys.* **27**, 1093-1100 (2000).
- 15 P. Karaiskos, A. Angelopoulos, L. Sakelliou, P. Sandilos, C. Antypas, L. Vlachos, E. Koutsouveli, "Monte Carlo and TLD dosimetry of an ¹⁹²Ir high dose-rate brachytherapy source," *Med Phys.* **25**, 1975-84 (1998).

- 16 D.M. Gearheart, A. Drogin, K. Sowards, A. S. Meigooni, and G.S. Ibbott, "Dosimetric characteristics of a new ¹²⁵I brachytherapy sources," *Med. Phys.* **27**, 1093-1100 (2000).
- 17 D. E. Lee, *Actions of Radiations on Living Cells* (London, Cambridge University Press, 1946)
- 18 G. W. Barendsen, "Dose fractionation, dose rate, and isoeffect relationships for normal tissue responses," *Int. J. Radiat. Oncol. Biol. Phys.* **8**, 1981-1997 (1982).

Table Captions

- Table 1A** Dose rates (cGy/MU) of 6 MV x-ray beam for a newly designed GRID block as a function of depth measured with TLD and film in Solid WaterTM and an ionization chamber in water for 10×10 cm field.
- Table 1B** Dose rates (cGy/MU) of 18 MV x-ray beam for a newly designed GRID block as a function of depth measured with TLD and film in Solid WaterTM and an ionization chamber in water for 10×10 cm field.
- Table 2A** Output factors as a function of field size and energy of the newly designed GRID block measured at d_{max} (1.5 cm for 6 MV and 2.5 cm for 18 MV) and 100 cm SSD with an ionization chamber in water as a function of field size and energy.
- Table 2B** Comparison of open field S_{c,p} with GRID relative outputs at d_{max} and 100 cm SSD as a function of field size and energy.
- Table 1A** Dose rates (cGy/MU) of 6 MV x-ray beam for a newly designed GRID block as a function of depth measured with TLD and film in Solid WaterTM and an ionization chamber in water for 10×10 cm field.

Methods	Depth (cm)	Dose Rate (cGy/MU)		Relative Dose Rate (%)
		Open area	Blocked area	Blocked-to- open area
TLD	1.5	0.89	0.12	13.5
	5.0	0.70	0.11	15.7
	10.0	0.55	0.11	20.0
Film	1.5	0.87	0.11	12.6
	5.0	0.70	0.12	17.1
	10.0	0.55	0.11	20.0
Ionization Chamber	1.5	0.89	0.12	13.5
	5.0	0.73	0.11	15.1
	10.0	0.54	0.10	18.5

Table 1B Dose rates (cGy/MU) of 18 MV x-ray beam for a newly designed GRID block as a function of depth measured with TLD and film in Solid WaterTM and an ionization chamber in water for 10×10 cm field.

Methods	Depth (cm)	Dose Rate (cGy/MU)		Relative Dose Rate (%)
		Open area	Blocked area	Blocked-to-open area
TLD	2.5	0.78	0.17	21.8
	5.0	0.73	0.18	24.7
	10.0	0.56	0.18	32.1
Film	2.5	0.78	0.15	19.2
	5.0	0.69	0.15	21.7
	10.0	0.57	0.14	24.6
Ionization-chamber	2.5	0.78	0.20	25.6
	5.0	0.73	0.20	27.4
	10.0	0.58	0.17	29.3

Table 2A Output factors as a function of field size and energy of the newly designed GRID block measured at dmax (1.5 cm for 6 MV and 2.5 cm for 18 MV) and 100 cm SSD with an ionization chamber in water as a function of field size and energy.

	Output Factor (cGy/MU)				
	5×5	10×10	15×15	20×20	25×25
6MV	0.88	0.89	0.91	0.92	0.93
18MV	0.75	0.78	0.81	0.83	0.84

Table 2B Comparison of open field S_{c,p} with GRID relative outputs at dmax and 100 cm SSD as a function of field size and energy.

		Field Size (cm ²)				
		5×5	10×10	15×15	20×20	25×25
6 MV	Relative Output factor	0.984	1.000	1.017	1.030	1.038
	S _{c,p}	0.940	1.000	1.034	1.059	1.073
18 MV	Relative Output factor	0.960	1.000	1.032	1.054	1.070
	S _{c,p}	0.921	1.000	1.041	1.065	1.078

Figure Captions

- Fig. 1** (a) the top view of a newly designed GRID block (b) photograph of the GRID block mounted on a Clinac 21EX linear accelerator.
- Fig. 2** Schematic diagram of the experimental setup for film dosimetry using 6MV and 18MV photon GRID fields.
- Fig. 3** Schematic diagram of the experimental setup for TLD (square symbol) dosimetry in a GRID radiation field.
- Fig. 4** Comparison of beam profiles for 6 MV x-ray obtained using film and ionization chamber dosimetry at depths of 1.5 cm (a) and 10 cm (b).
- Fig. 5** Comparison of transverse profiles from film dosimetry for newly designed and prototype GRID for a 10x10 cm field at the depth of maximum dose in Solid WaterTM phantom material using (a) 6MV and (b) 18MV x-ray irradiation.
- Fig. 6** Comparison of transverse profiles from film dosimetry for an open field and a GRID field for a 10x10 cm field at the depth of maximum dose in Solid WaterTM phantom material using (a) 6MV and (b) 18MV x-ray irradiation.
- Fig. 7** Dose distribution (a) and isodose curves (b) obtained from 6MV GRID x-ray irradiation using film dosimetry technique at d_{max} for a 10x10cm field size.
- Fig. 8** Comparison of profiles between 6 MV and 18 MV photons from film dosimetry at the depth of maximum dose at a field size of 10x10 cm.
- Fig. 9** Depth dependence of (a) crossplane and (b) inplane profiles obtained from ionization chamber measurements for 6 MV GRID x-ray beams at 10x10 cm field size.
- Fig. 10** Depth dependence of (a) crossplane and (b) inplane profiles obtained from ionization chamber measurements for 18 MV GRID x-ray beams at 10x10 cm field size.
- Fig. 11** Percent depth dose (%DD) for a 10x10 cm field along the depth axis of the central aperture for GRID collimated fields of (a) 6 MV and (b) 18 MV x-ray beams. %DD data were obtained from ionization chamber measurements in water and film and TLD measurements in Solid WaterTM phantom material.
- Fig. 12** Percent depth dose (%DD) as a function of field sizes for 6 MV and 18 MV x-ray beams in water phantom.
- Fig. 13** Representative grid dose profile under one hole (a), integrated dose area histogram (b), and differential dose area histogram (c) at d_{max} for a 6 MV x-ray beam.
- Fig. 14** Calculation of therapeutic advantage of normal cells for a GRID field versus an open uniform field as a function of dose.



(a)



(b)

Fig. 1 (a) the top view of a newly designed GRID block (b) photograph of the GRID block mounted on a Clinac 21EX linear accelerator.

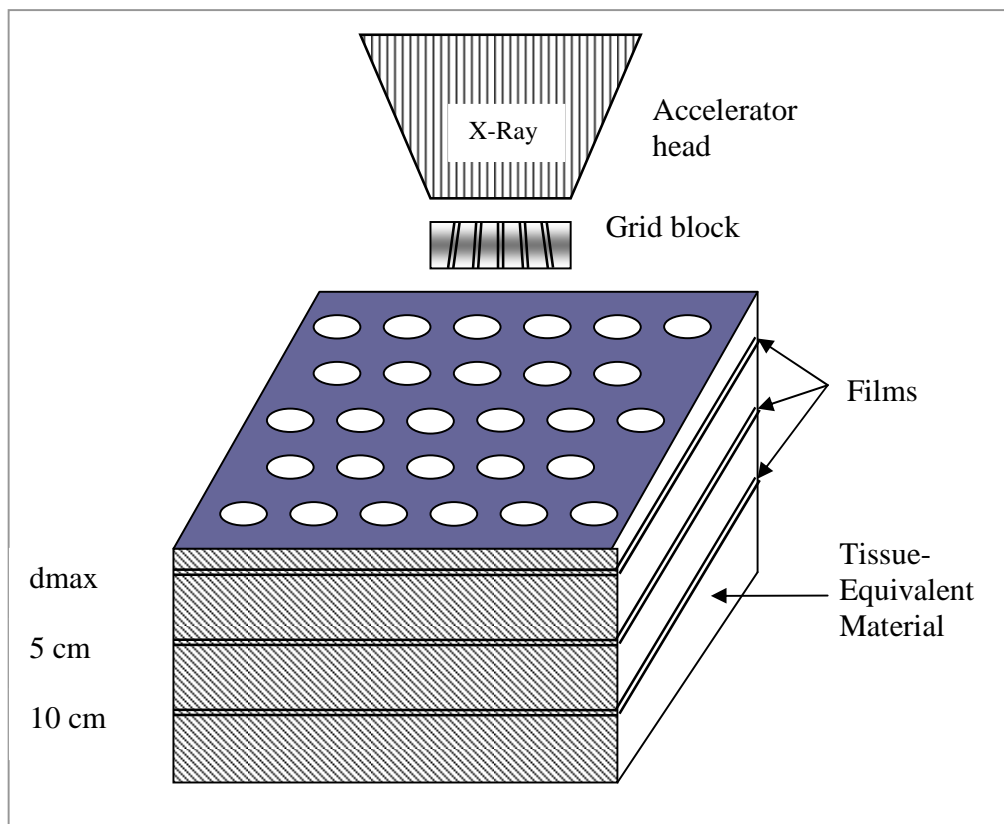


Fig. 2 Schematic diagram of the experimental setup for film dosimetry using 6 MV and 18 MV photon GRID fields.

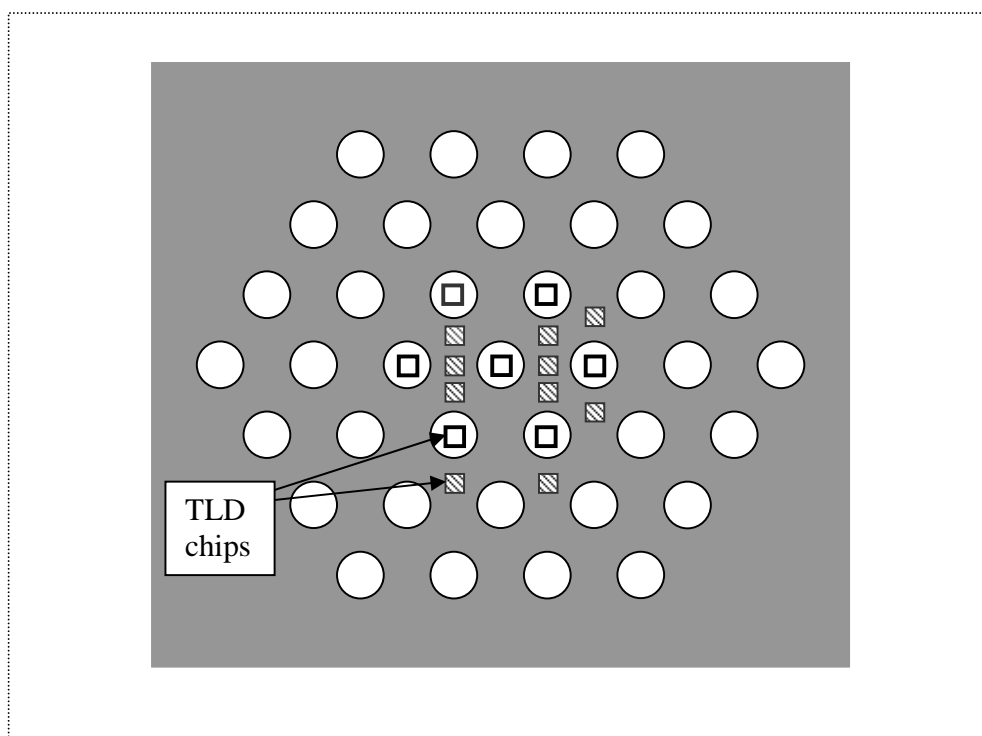
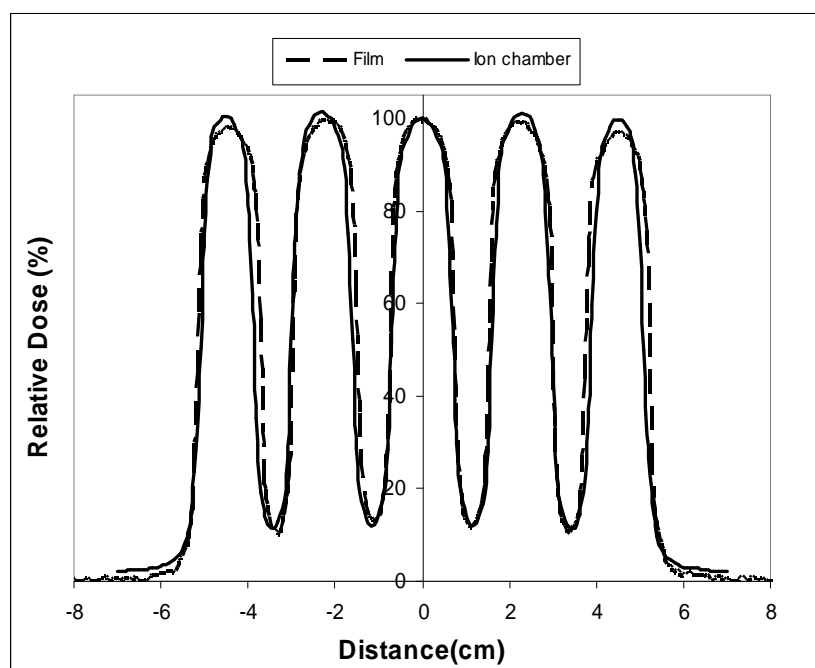
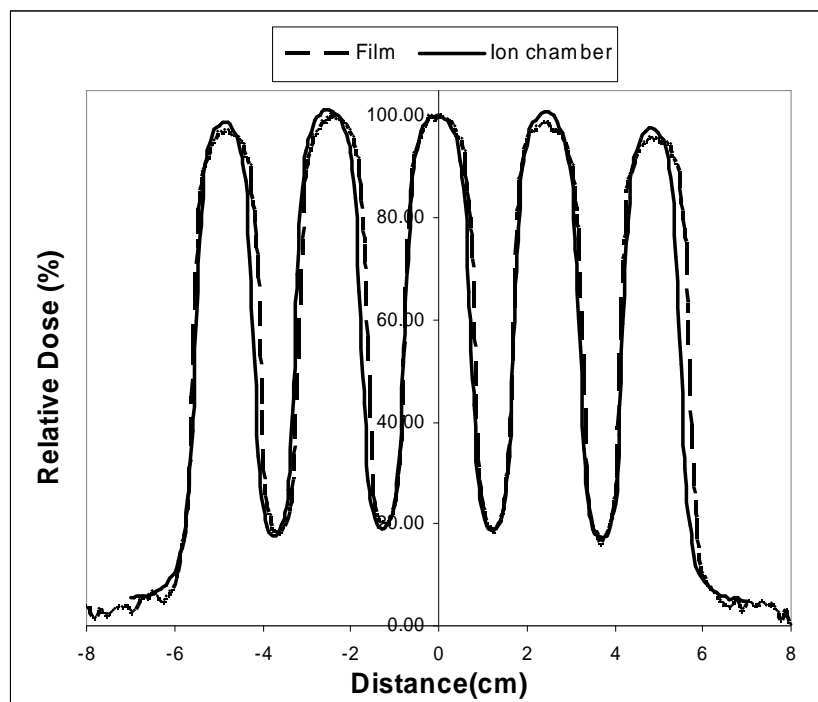


Fig. 3 Schematic diagram of the experimental setup for TLD (square symbol) dosimetry in a GRID radiation field.

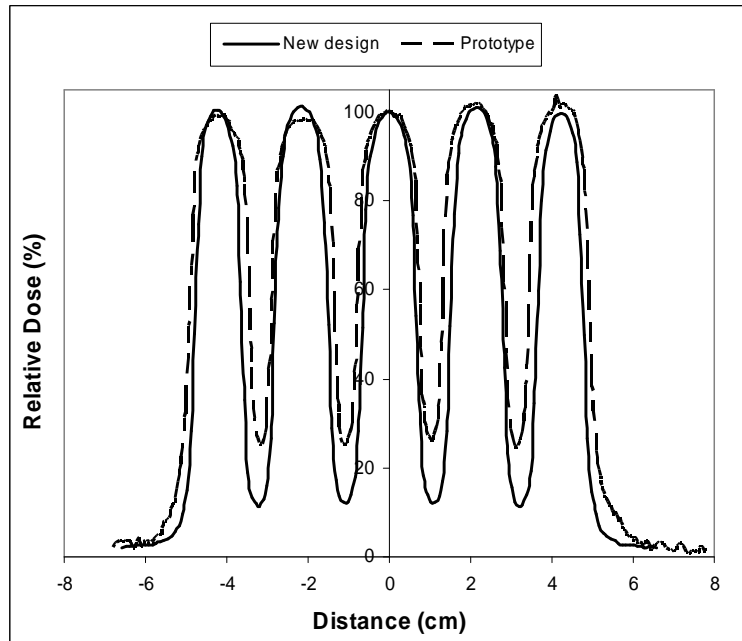


(a)

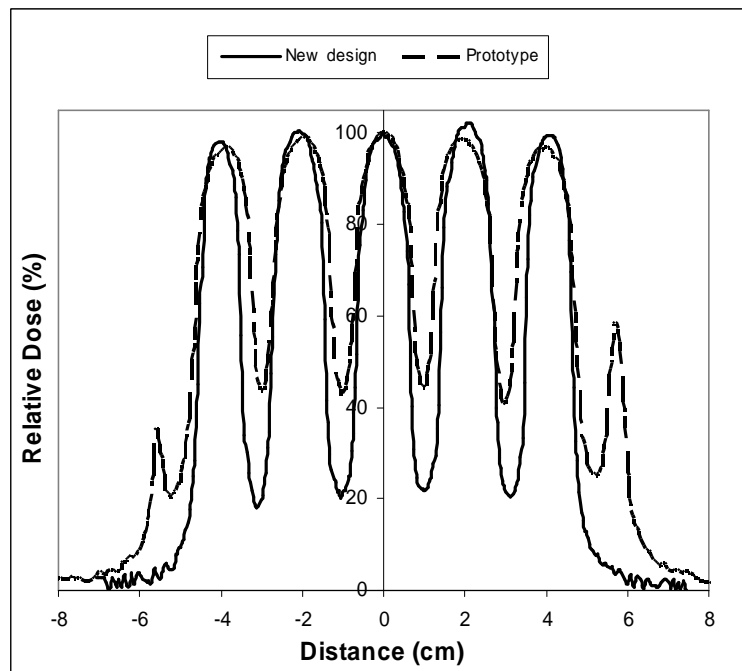


(b)

Fig. 4 Comparison of beam profiles for 6 MV x-ray obtained using film and ionization chamber dosimetry at depths of 1.5 cm (a) and 10 cm (b).

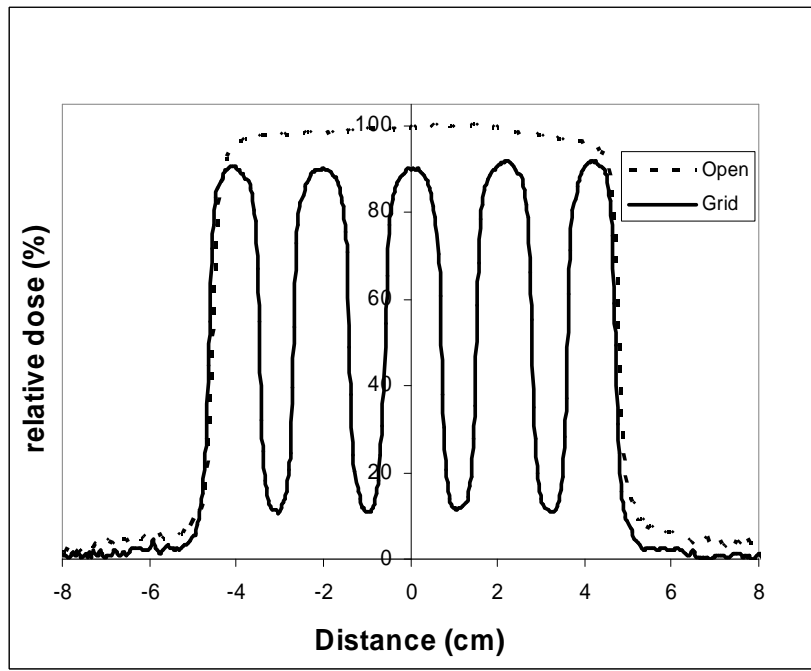


(a)

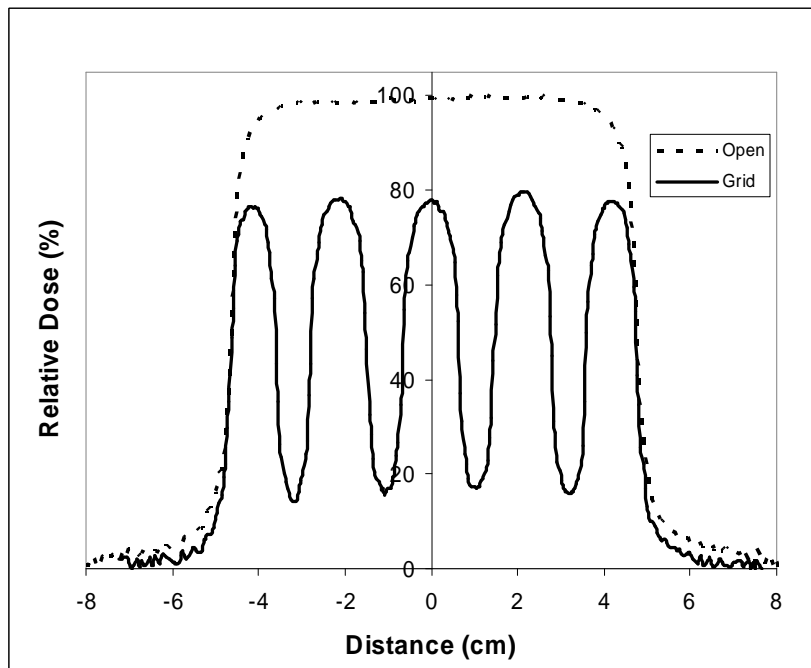


(b)

Fig. 5 Comparison of transverse profiles from film dosimetry for newly designed and prototype GRID for a 10x10 cm field at the depth of maximum dose in Solid WaterTM phantom material using (a) 6MV and (b) 18MV x-ray irradiation.

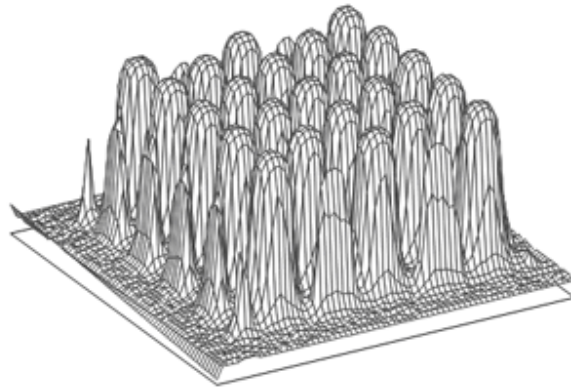


(a)

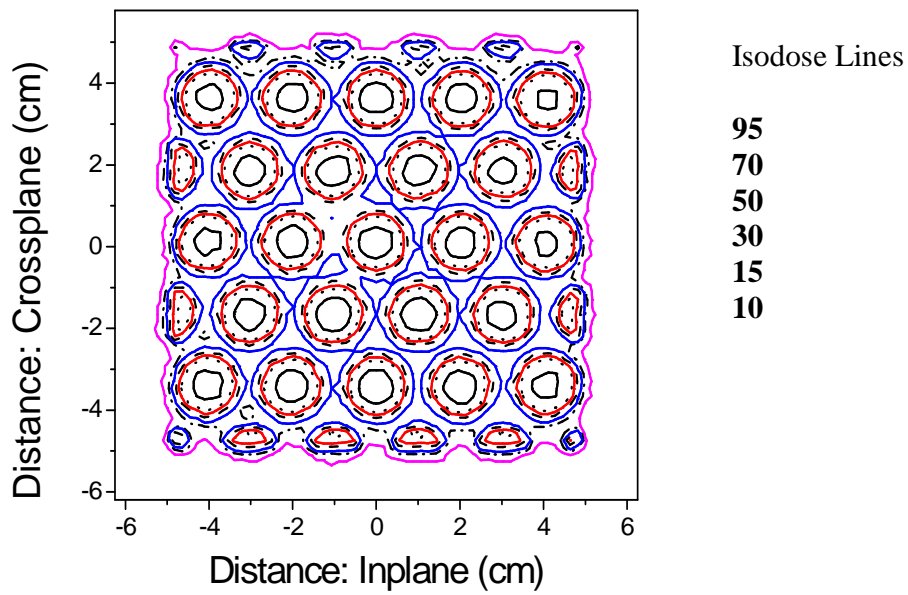


(b)

Fig. 6 Comparison of transverse profiles from film dosimetry for an open field and a GRID field for a 10x10 cm field at the depth of maximum dose in Solid WaterTM phantom material using (a) 6MV and (b) 18MV x-ray irradiation.



(a)



(b)

Fig. 7 Dose distribution (a) and isodose curves (b) obtained from 6MV GRID x-ray irradiation using film dosimetry technique at d_{max} for a 10×10cm field size.

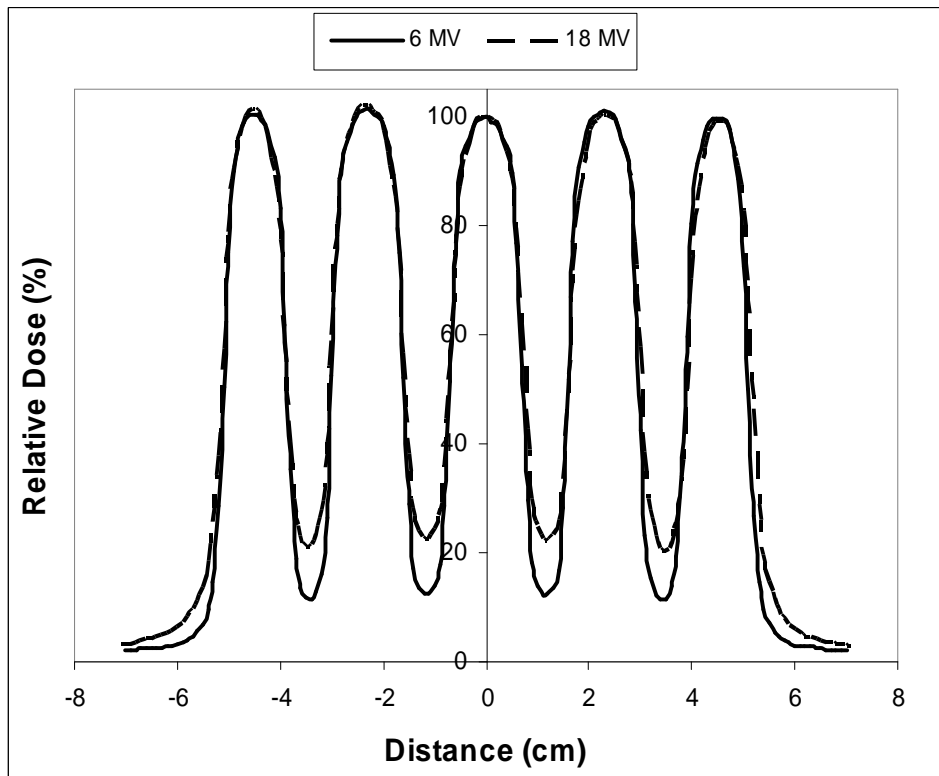
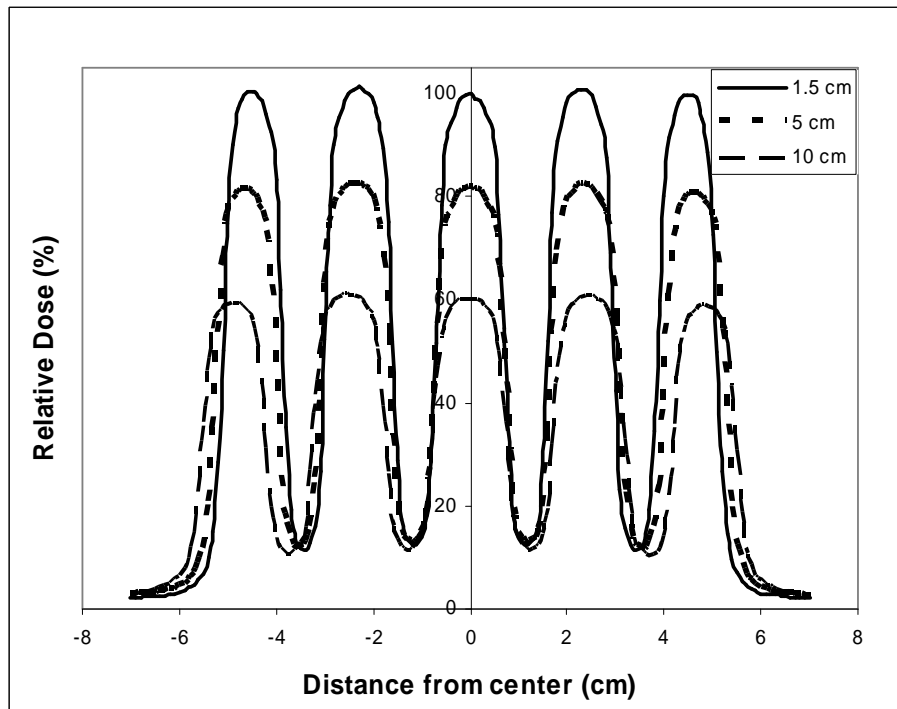
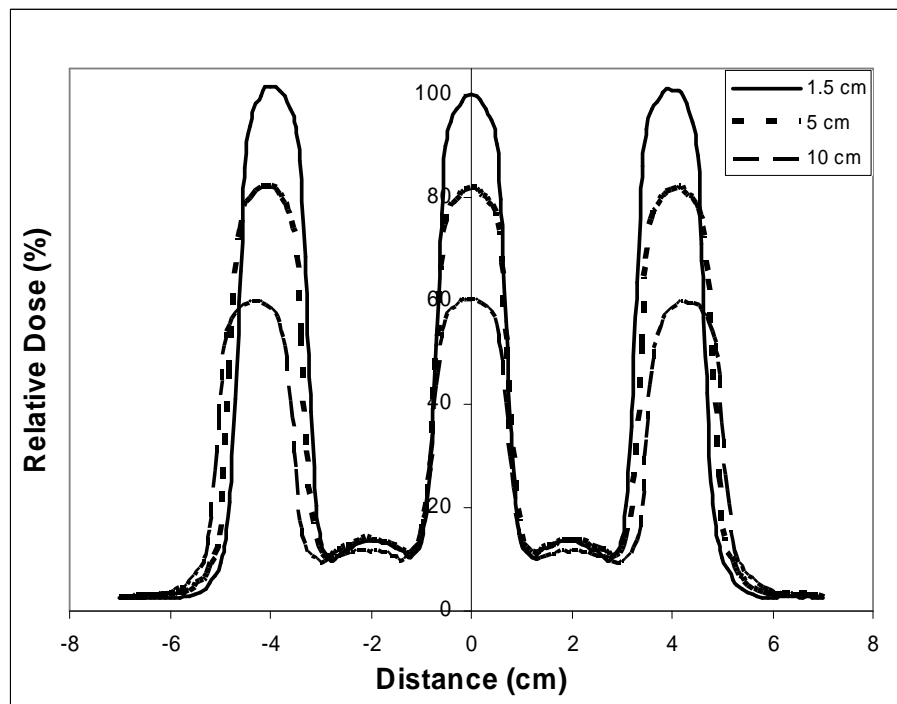


Fig. 8 Comparison of profiles between 6 MV and 18 MV photons from film dosimetry at the depth of maximum dose at a field size of 10x10 cm.

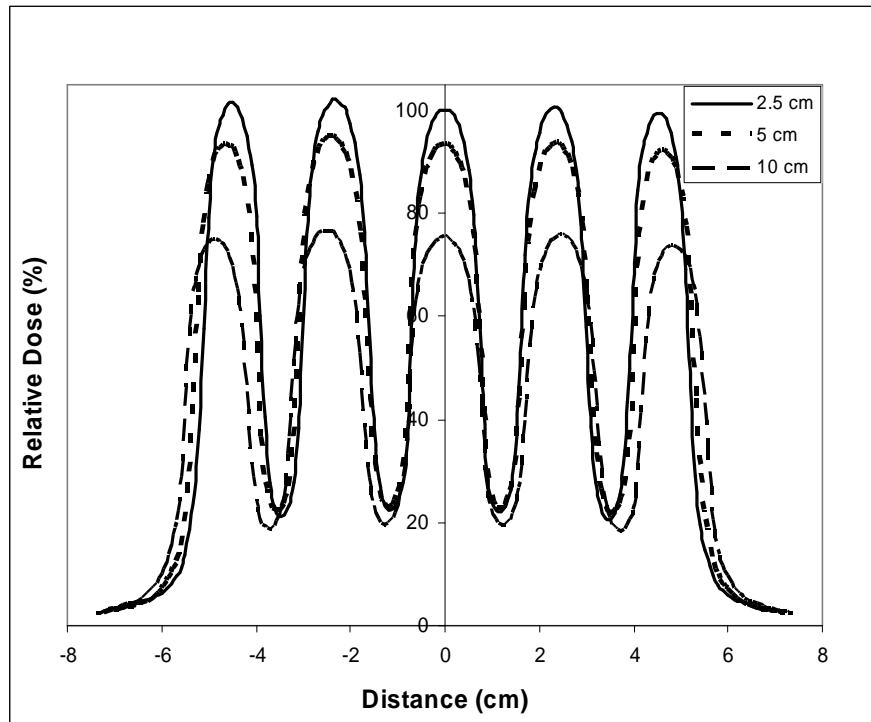


(a)

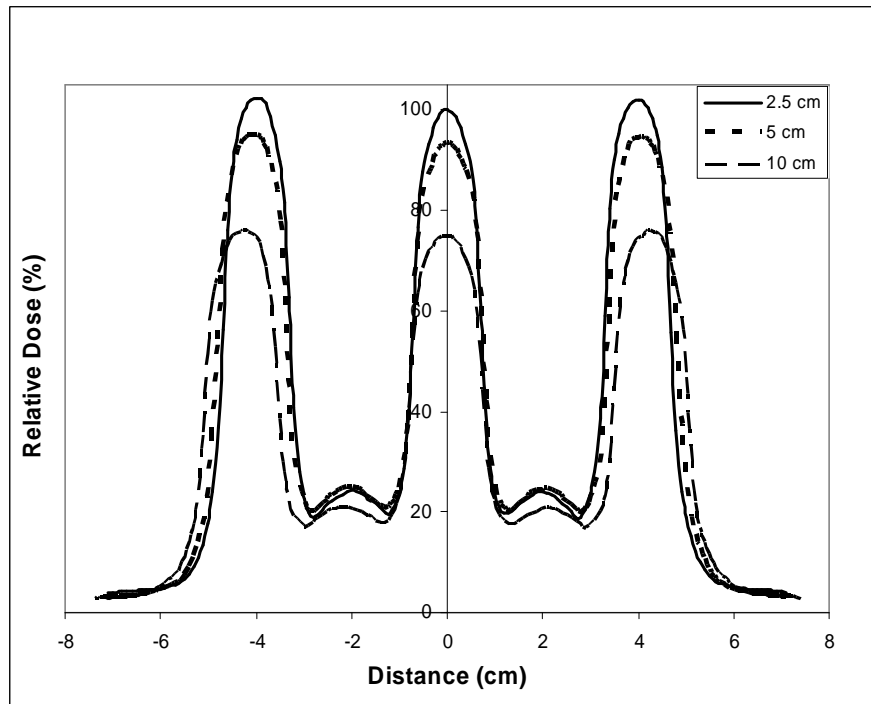


(b)

Fig. 9 Depth dependence of (a) crossplane and (b) inplane profiles obtained from ionization chamber measurements for 6 MV GRID x-ray beams at 10x10 cm field size.

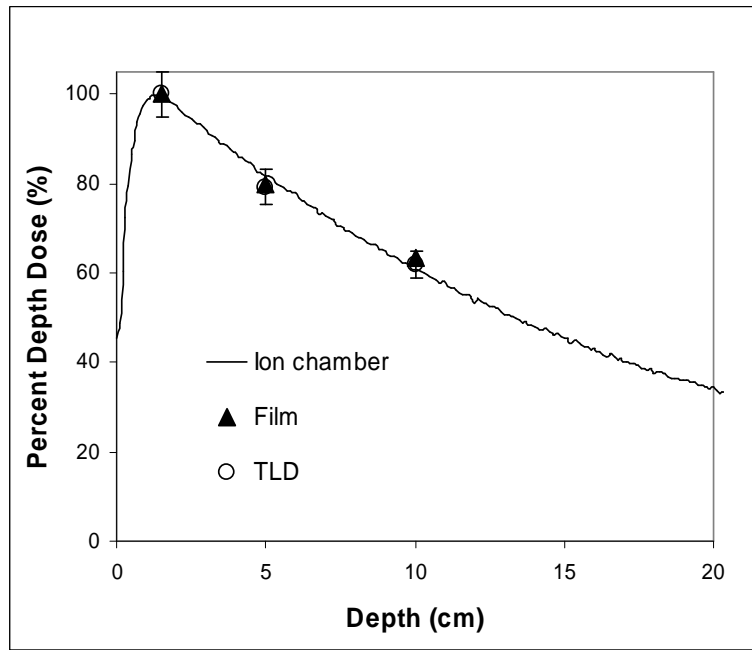


(a)

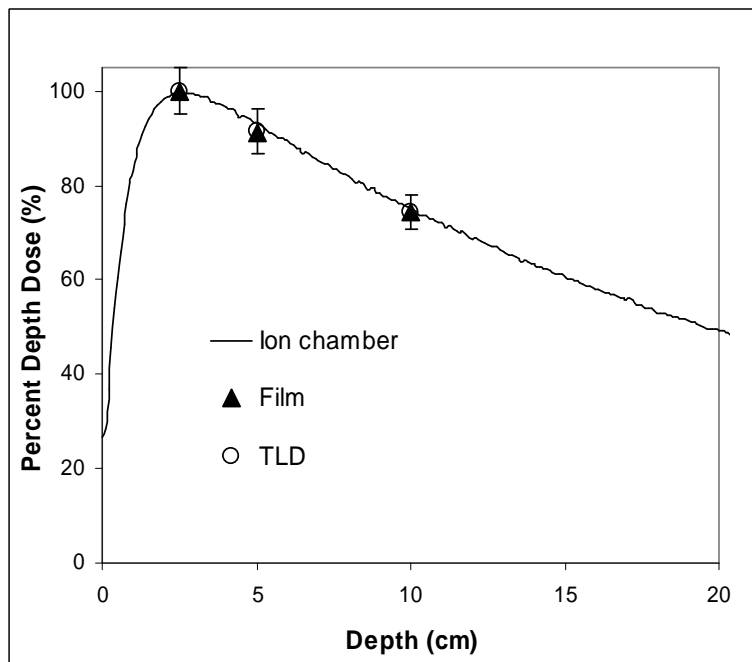


(b)

Fig. 10 Depth dependence of (a) crossplane and (b) inplane profiles obtained from ionization chamber measurements for 18 MV GRID x-ray beams at 10x10 cm field size.

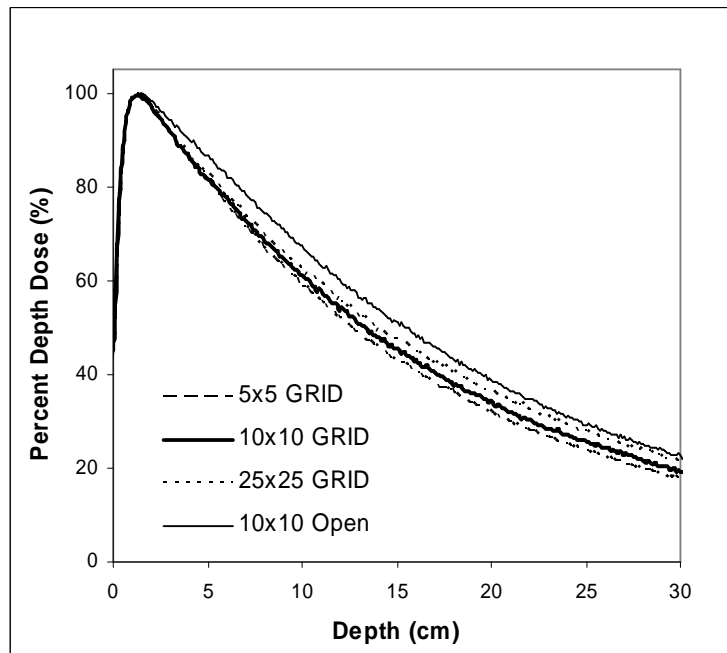


(a)

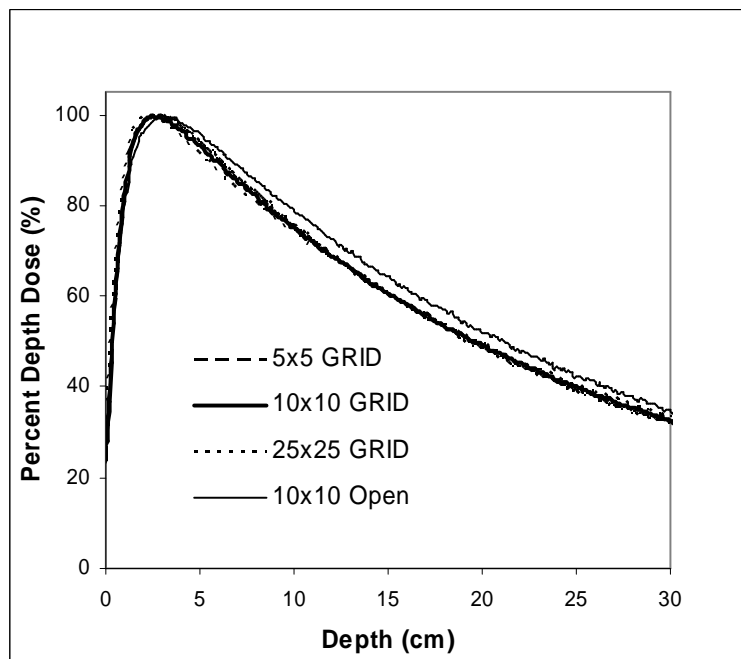


(b)

Fig. 11 Percent depth dose (%DD) for a 10×10 cm field along the depth axis of the central aperture for GRID collimated fields of (a) 6 MV and (b) 18 MV x-ray beams. %DD data were obtained from ionization chamber measurements in water and film and TLD measurements in Solid WaterTM phantom material.



(a)



(b)

Fig. 12 Percent depth dose (%DD) as a function of field sizes for (a) 6 MV and (b) 18 MV x-ray beams in water phantom.

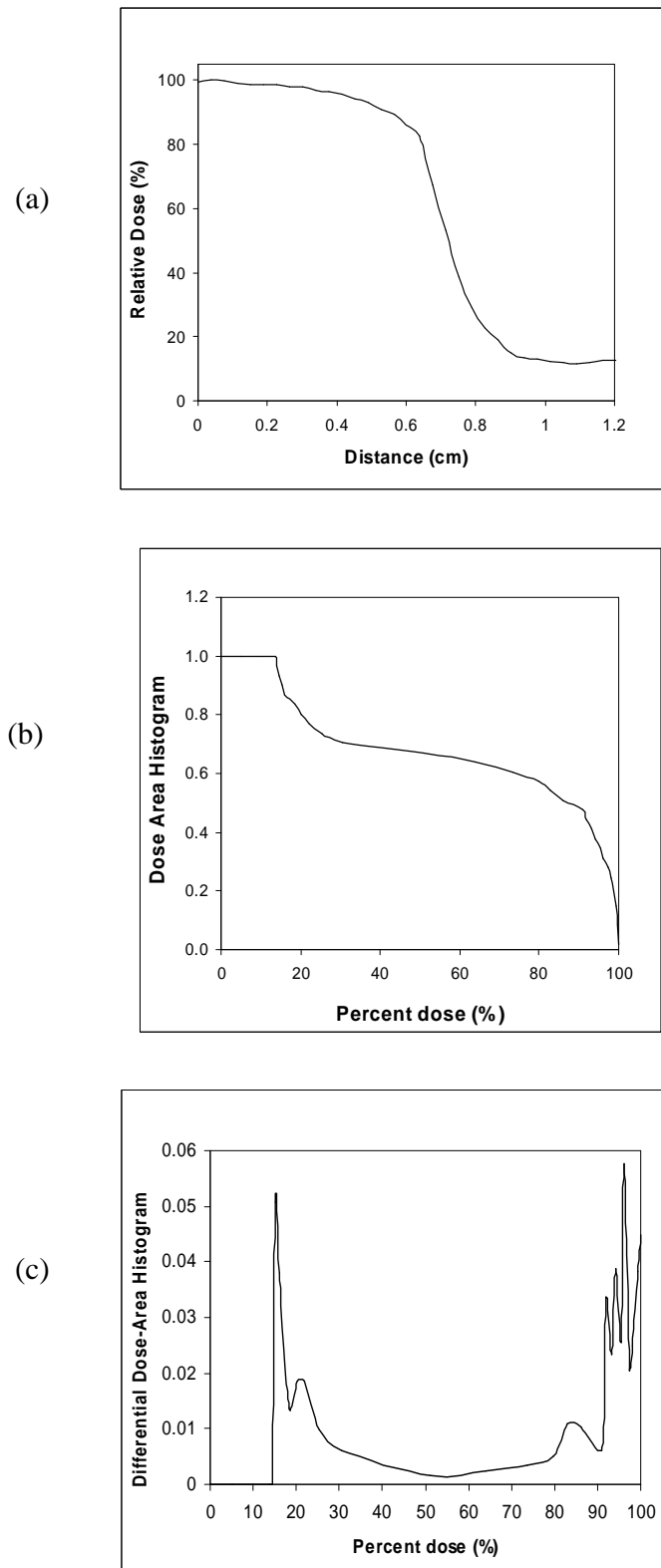


Fig. 13 Representative grid dose profile under one hole (a), integrated dose area histogram (b), and differential dose area histogram (c) at d_{max} for a 6 MV x-ray beam.

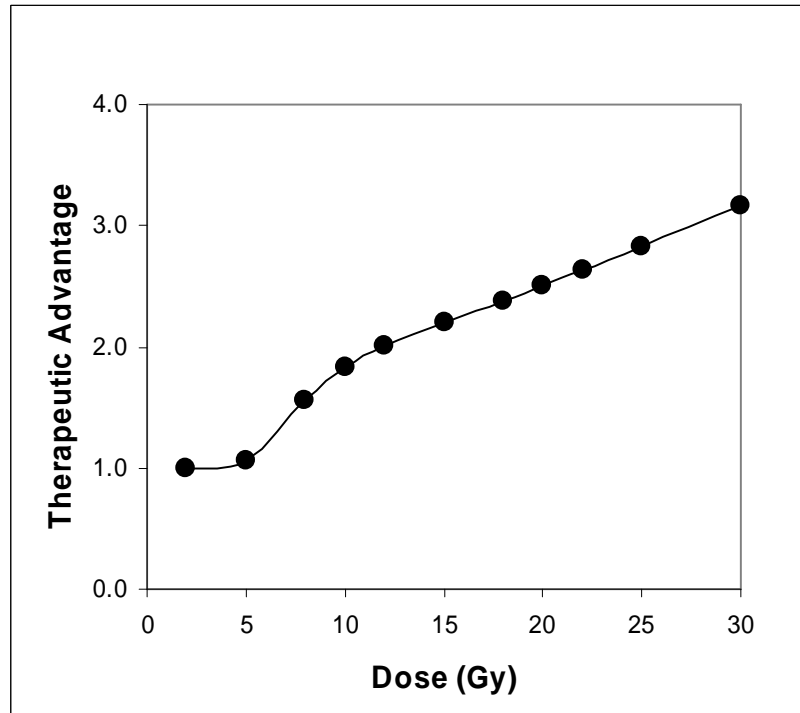


Fig. 14 Calculation of therapeutic advantage of GRID field versus an open uniform field as a function of absorbed dose.